First-Principles Prediction of Room Temperature Ferromagnetic Janus VSSe Monolayer with Ferroelasticity, Large Valley/Piezoelectric Polarization

Chunmei Zhang[1], Yihan Nie[1], Stefano Sanvito[2] and Aijun Du[1,]*

[1]School of Chemistry, Physics and Mechanical Engineering, Queensland University of Technology, Gardens Point Campus, Brisbane, QLD 4001, Australia

[2]School of Physics, AMBER and CRANN Institute, Trinity College, Dublin 2, Ireland

Inspired by recent experiments on the successful fabrication of monolayer Janus transition metal dichalcogenides [*Nat. Nanotechnol. 12 (2017) 744]* and ferromagnetic VSe_2 [*Nat. Nanotechnol. 13 (2018) 289*], here we for the first time predict a highly stable room temperature ferromagnetic Janus monolayer (VSSe) by ab initio evolutionary and density functional theory methods. Monolayer VSSe exhibits a large valley polarization due to the broken space and time-reversal symmetry. Moreover, the low symmetry C3v point group of VSSe monolayer results in giant in-plane piezoelectric polarization. Most interestingly, a strain-driven 90° lattice rotation is occurred in magnetic VSSe monolayer with an extremely high reversal strain (73%), indicating an intrinsic ferroelasticity. The combination of multiferroic, piezoelectricity, and valley polarization will render magnetic 2D Janus VSSe for potential applications in nanoelectronics, optoelectronics and valleytronics.

As the technological aspirations for the miniaturization of multifunctional electronics and information storage, integrating multiple electronic functionality in one nanomaterial is highly demanded [1,2]. Two dimensional (2D) multiferroic exhibiting more than two ferroic properties: ferromagnetism, ferroelasticity, and ferroelectricity [3], has been proposed to replace silicon based electronics [4]. Additionally, electromechanical coupled devices that are piezoelectric have also attracted great research interests recently as it exhibits switchable electrical polarization under mechanical strain with potential applications in sensors, power generation and electronics [5-7]. To search compounds that couple magnetic, mechanical, and electric, great efforts have been made in studying geometrical symmetry that leads to novel material properties in the presence of external operations. Generally, materials without centrosymmetry possesses intrinsic polarization domains and are piezoelectric, such as ZnO, GaN, transition-metal dichalcogenides (TMD)[8]. Materials with spontaneous deformation or magnetization can be switchable by an external strain or magnetic field and are ferroelastic or ferromagnetic [3]. However, rare 2D materials have both intrinsic ferroelasticity and ferromagnetic, and the 2D materials that could couple magnetic-mechanical-electric interactions are even more scarce. So far, there are no reported 2D materials that can exhibit both intrinsic ferroelasticity and ferromagnetic at room temperature.

Recently, the experimentally synthesised Janus TMD monolayer [5] has attracted great research interests because it can harbour both in-plane and mirror asymmetry. The Janus monolayer TMD not only preserves the valley properties (inequivalent valley Berry curvature) compared to that of conventional TMD systems, but also possesses Rashba effect, spontaneous out-of-plane dipole, as well as large intrinsic piezoelectric effect [5] . However, magnetism is absent in all the reported Janus systems including MoSSe, WSSe, WSeTe, and WSTe [9]. And energy valley is protected by the Berry curvature and orbital magnetic moment, i.e. time-reversal symmetry [10]. In the Janus materials, contrasting Berry curvature is generated as the inversion symmetry is broken, while an external magnetic field [11] could lead to the violation of time-reversal symmetry, thus lifting valley degeneration. A magnetic Janus monolayer fully fulfils these requirements. Most recently, a 2D magnetic VSe_2 [12] is successfully fabricated in experiment. One open question is whether we can introduce broken mirror symmetry into VSe_2 by designing a magnetic Janus VSSe monolayer? Magnetic VSSe might be an excellent multiferroics if proved to be energetically and dynamically stable.

In this work, we for the first time predict a new room temperature ferromagnetic Janus VSSe monolayer by particle swarm optimization (PSO) and first-principles approaches. 1T and 2H ferromagnetic Janus VSSe monolayers are first identified to be the most stable phases. Time-reversal symmetry is violated by an intrinsic magnetic field which is induced by the combination of the spin-orbit-coupling (SOC) and exchange interaction of $d_{x^2-y^2}$/ d_{xy} and d_{z^2} orbital of V. A large direct valley polarization (~85meV) is predicted and further validated by a $k \cdot p$ model. Compared with monolayer VSe_2, in which the polarization is forbidden due to mirror symmetry, the magnetic Janus VSSe monolayer possesses an intrinsic out-of plane dipole moment, thus leading to a large vertical piezoelectric polarization. When Janus VSSe is subjected to a uniaxial in-plane strain, a giant in-plane piezoelectric effect ($3.303*10^{-10}$C/m) is generated. Remarkably, novel ferroelasticity is demonstrated in the magnetic Janus VSSe monolayer with an ultrahigh reversible strain up to 73% which is much higher than that reported in other 2D materials [13], indicating extremely strong signal of switching.

Structural search for 2D magnetic VSSe in the ground state were carried out by using the particle swap method as implemented in the CALYPSO code[14]. The electronic structure calculations were performed using density functional theory (DFT) within generalized gradient approximation of the Perdew−Burke−Ernzerhof (PBE) functional by *the* Vienna ab initio simulation package (VASP) [15-17]. The hybrid functional method based on the Heyd−Scuseria−Ernzerhof (HSE) exchange−correlation functional [18] was adopted for accurately calculating band structure. A long-range van der Waals interaction (DFT-D3 method) was incorporated to correct total energy [19]. A vacuum layer with a thickness of 15 Å is used to avoid artificial interactions between neighbouring layers and. The energy cut-off of 500 eV is set for a plane-wave basis set. The monolayer VSSe was relaxed until energy and force were converged to 10^{-6} eV and 0.001eV/Å. The Monkhorst−Pack k-point meshes are 19 × 19 × 1 for sampling the Brillouin zone. The SOC effect is also considered in this calculation. To explore the dynamical stability of VSSe monolayer, phonon dispersion was obtained by using the finite displacement method [20] as implemented in the Phonopy code[21]. Ab initio molecular dynamics (AIMD) simulations with canonical ensemble were performed to evaluate the thermodynamic stability and electric polarizations are computed by using the Berry phase method [22].

Low-energy Janus VSSe monolayer are first predicted to be in the 1T and 2H phases (see Fig. 1a and Fig1.c) by particle swarm search method with 3 atoms in a hexagonal unit cell. Both phases adopted C3v symmetry and the lattice constants/total energies are calculated to be 3.25Å/-

19.24eV and 3.24Å/-19.31eV for 1T and 2H VSSe monolayers, respectively. VSSe monolayer is ferromagnetic and 2H VSSe is more stable than 1T phase as shown in Table s1. Figure 1b and 1d presented the calculated phonon spectrum for the 1T and 2H phase VSSe monolayers, respectively. Clearly, there is no imaginary frequency, indicating high dynamical stability. AIMD simulations were further carried out for 10ps at 300K and 1000K as shown in Fig. s1. There is no structural destruction, suggesting the robust thermal stability for monolayer VSSe. It is important to note that Janus MoSSe monolayer has been recently fabricated using CVD methods[5,23]. The experimental realization of magnetic Janus VSSe monolayer is expected to be straightforward using a similar approach for the synthesis of MoSSe.

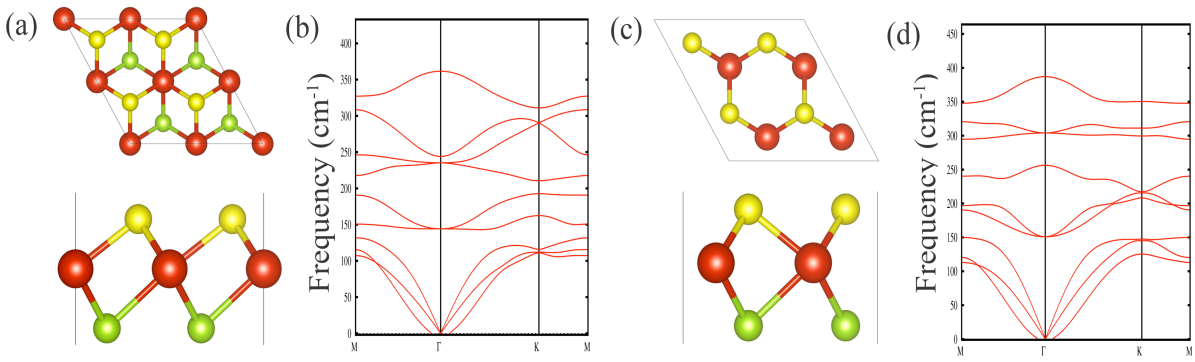

Figure 1 The atomic structures in a 2×2×1 supercell and phono spectrum for the (a-b) 1T and (c-d) 2H VSSe monolayer. Yellow, red, and green balls represent S, V, and Se atoms, respectively.

After confirming the stability of magnetic Janus VSSe monolayers at an elevated temperature, we further move to check if the ferromagnetic could survive at room temperature. The Curie temperature T_C can be estimated by the mean-field approximation (MFA) and Heisenberg model [24,25]. T_C is expressed as $T_C = \frac{2}{3*K_B}J$, J is the exchange coupling parameter (more details can be found in Supplemental Material). Here we mainly focus on the study of 2H monolayer VSSe as it is the most energetically stable. The calculated T_C for 2H VSeS is around 354K, which is much higher than the transition temperatures observed in exfoliated 2D ferromagnetic CrI_3 [26] and $CrGeTe_3$ [27]. Thus, an intrinsic magnetic field in 2H VSeS monolayer could persist around room temperature.

Then the electronic properties of 2D magnetic Jannus VSSe monolayer were accurately calculated by hybrid functional method. The spin-resolved band structures with and without SOC for the 2H monolayer VSSe and metastable 1T phase VSSe are presented in Fig. 2 and Fig. s2, respectively. In addition, calculations based on standard PBE functional (see Fig. s3a-b) were also carried out for

comparison. Direct spin-up and spin-down gaps are predicted by HSE method to be 0.96eV and 1.51eV for 2H VSSe monolayer (Fig. 2a). Interestingly, a valley polarization is present at the K and K' points (see Fig. 2b) when the SOC effect is incorporated. The valley energy difference between K and K' is around 85 meV at valence band maximum (VBM), which is mainly contributed by the dxy/dx^2-y^2 orbitals of V atoms (see red circle in Fig. 2c). While conduction band minimum (CBM) is dominated by the dz^2 orbital of V atoms (see green circle in Fig. 2c), which should corresponds to a small band energy splitting.

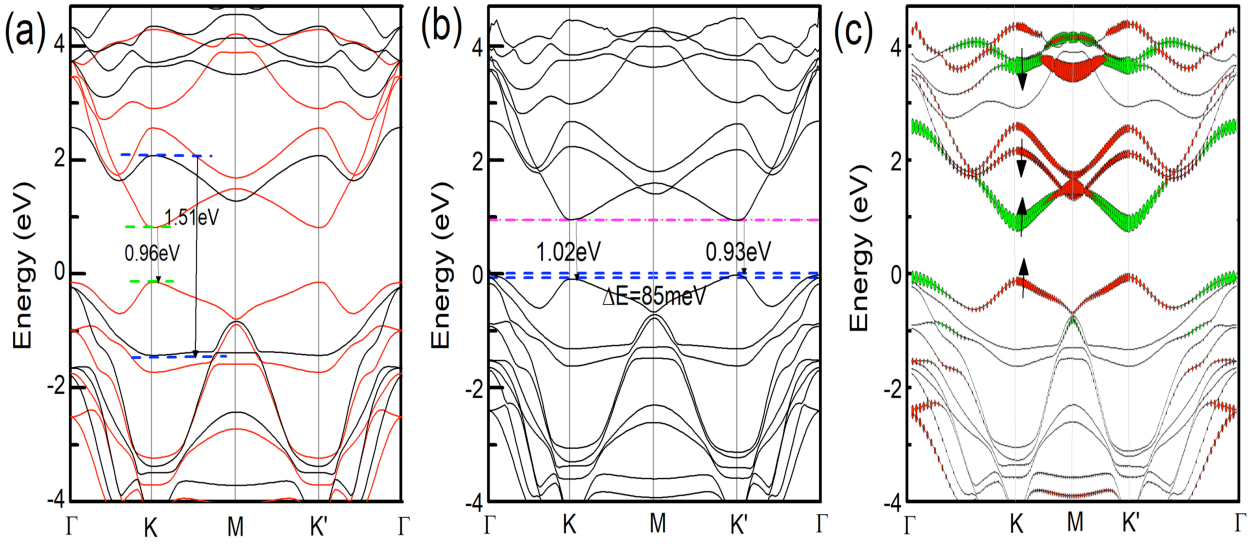

Figure 2 The spin-polarized band structures of 2H magnetic Janus VSSe monolayer (a) without and (b) with SOC by HSE method. The red and black lines represent spin up and spin down band structures in Fig 2 (a). Fig 2 (c) presents the orbital resolved band structure with SOC, and red circle denotes contribution from dxy/dx^2-y^2 of V atoms, while green circle is from dz^2 orbital of V atoms. As can be seen in the Fig. 2 (c), black arrows with up and down directions represent bands from spin up and spin down electrons respectively. Thus four bands are arising from spin up dxy/dx^2-y^2 orbital, spin up dz^2 orbital, spin down dxy/dx^2-y^2 orbital, and spin down dz^2 orbital of V atom, respectively. The Fermi level is set to zero in each figure.

The valley polarization can be further understood from a simplified 4 x 4 $k \cdot p$ model [28]. The basic functions are choose as $|\Psi_{CB}^{\tau}\rangle = |d_{z^2}\rangle$ and $|\Psi_{VB}^{\tau}\rangle = (|d_{x^2-y^2}\rangle + i\tau |d_{xy}\rangle)/\sqrt{2}$. Carriers in K and K' valleys in inversion asymmetry systems, belong to opposite Berry curvatures [20], thus τ = ±1 represents the valley index of K and K' in magnetic VSSe monolayer. (more details can be found in the Supplemental Material). By incorporating nearest-neighbours hopping parameter t_{12}. The Hamilton can be written as,

$$H = \begin{bmatrix} \frac{\Delta}{2} + \epsilon - m_{VB} & t_{12}(\tau k_x - i k_y) & 0 & 0 \\ t_{12}(\tau k_x + i k_y) & -\frac{\Delta}{2} + \epsilon + \tau\lambda - m_{CB} & 0 & 0 \\ 0 & 0 & \frac{\Delta}{2} + \epsilon + m_{VB} & t_{12}(\tau k_x - i k_y) \\ 0 & 0 & t_{12}(\tau k_x + i k_y) & -\frac{\Delta}{2} + \epsilon - \tau\lambda + m_{CB} \end{bmatrix} \quad (1)$$

Δ is the bandgap at the valleys (K and K'), ϵ is the correction energy relevant to the Fermi energy, t_{12} is the effective nearest neighbor hopping parameter. And $\mathrm{k} = \mathbf{k} - \mathbf{K}$ is the momentum vector. The SOC-induced spin splitting at CBM (VBM), $2\lambda_{CB}(2\lambda_{VB})$, is defined by the energy difference $E_{CB(VB)\uparrow} - E_{CB(VB)\downarrow}$ at the K and K' point. The $-m_{CB}(-m_{VB}) = E_{CB(VB)\downarrow} - E_{CB(VB)\uparrow}$ represents the effective exchange splitting in the band edge of CB (VB). The fitted four bands (which are contributed by spin up dxy/dx^2-y^2 orbital, spin up dz^2 orbital, spin down dxy/dx^2-y^2 orbital, and spin down dz^2 orbital of V atom) at K and K' near Fermi surface based on DFT results are given in Fig. s4 (b). By incorporating SOC and the exchange interaction in the $k \cdot p$ model, the valley polarization is around 83meV at VBM, which is close to the HSE results. Thus, our $k \cdot p$ model captured well the valley polarization in magnetic Janus VSSe monolayer due to the strong coupling between spin and valley index.

As shown in Fig. 1, the length of V-S chemical bond is shorter than that of V-Se, and the angles between S-V-S and Se-V-Se are different (more details in Fig. s5). The anisotropic bonding shears the structure and lowers the structure symmetry, which would render spontaneous deformation in 2H VSSe. To explore this effect, we further investigated the magnetic Janus VSSe monolayer in the presence of mechanical strain. Fig.3 presented the change of energy as function of uniaxial strain in 2H magnetic Janus VSSe monolayer. Clearly there is a spontaneous deformation switched by external strain, suggesting an intrinsic ferroelasticity. As shown in Fig. 3, the initial state I represented a parallel armchair and zigzag rows lie in a and b direction, and the lattice constant a in armchair direction is more than b in zigzag direction (Table s2). When a uniaxial strain is imposed along b (zigzag) direction in magnetic Janus VSSe monolayer, it transformed into the configuration III which is energetically more favourable. The lattice parameters (a and b) are exchanged and the parallel zigzag rows are switched to a direction under state III, which is similar to the initial structure I with 90° rotation. The displayed configuration II with a square lattice is supposed to be the intermediate state between I and III, with optimized lattice constants a' = b' = 4.31Å (Table s2). Due to the symmetry, the reaction path from II to I and from II to III is nearly the same. The calculated energy barrier is approximately 0.23 eV/atom in 2H VSeS, which is low enough to make room temperature ferroelasticity available[13]. Another key indicator on the ferroelastic performance is the strength of reversible ferroelastic strain that controls the signal intensity and is defined as $(\frac{b}{a} - 1) \times 100\%$. The calculated reversible ferroelastic strain for magnetic Janus 2H VSSe monolayer is as high as 73%. It should be noted that the highest reversible ferroelastic strain that achieved up to date among 2D materials is 37.9% in

phosphorene [13]. The enormous reversible strain in magnetic Janus 2H VSSe monolayer indicate extremely strong signal of switching.

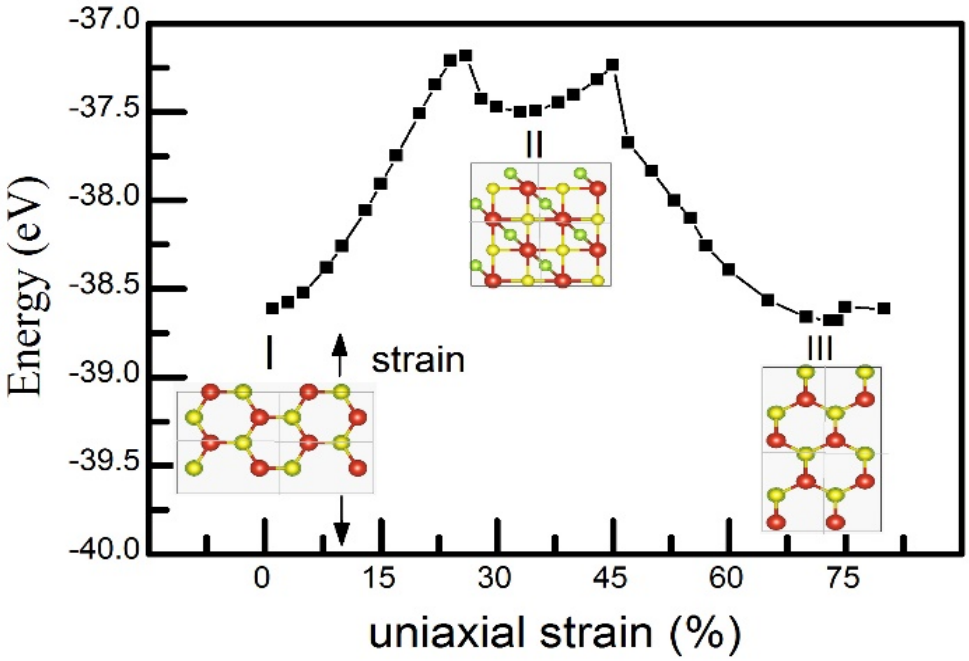

Figure 3 Pathway of ferroelastic switching (I-II-III) for 2H VSSe monolayer, where yellow, red, and green spheres denote S, V, Se atoms, respectively. The energy profiles of ferroelastic switching as a function of uniaxial strains in b (zigzag) direction. The inset shows top view of the 2 x 2 x 1 supercell structure of VSSe monolayer.

Magnetic Janus VSSe possesses crystal asymmetry, suggesting it to be piezoelectric. The piezoelectric effect is the coupling between electrical polarization (P_i) and strain (ε_{jk}) tensor described by third-rank tensors $e_{ijk} = \partial P_i / \partial \varepsilon_{jk}$, where i, j, and k correspond to the x, y, and z directions[7]. On the basis of symmetry analysis, magnetic Janus VSSe monolayer (space group C3v) should exhibits two non-zero independent piezoelectric coefficient. The DFT calculations are performed with respect to an unstrained state as a reference. Uniaxial strain is applied along the armchair direction up to 1.5% and the polarization is estimated by using the Berry-phase method [22] for both the unstrained and strained cases in the magnetic Janus VSSe. Fig. 4 presented the in-plane (e_{11}) and out-of plane (e_{13}) piezoelectric coefficients of the monolayers VSSe as a function of uniaxial strain along armchair direction. The value of e_{11} for magnetic Janus VSSe is calculated to be $3.303*10^{-10}$ C/m, which is much larger than that of MoS_2 monolayer with e_{11} of $2.900*10^{-10}$ C/m in experiment [7,8]. The estimated out-of plane piezoelectric coefficient e_{13} in 2H VSSe monolayer is about $0.948*10^{-10}$ C/m, which is relatively weaker than the in-plane piezoelectric effect. It should be noted that rare 2D materials have out-of plane piezoelectric polarization.

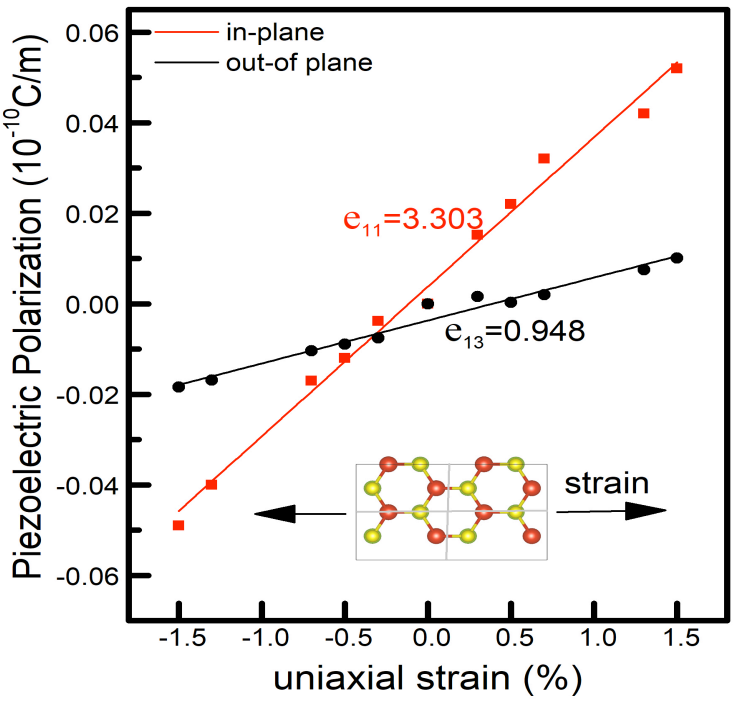

Figure 4 linear changes in in-plane and out-of-plane piezoelectric polarizations of the 2H VSSe monolayer under uniaxial strain (armchair) between −1.5% and 1.5%, giving its e_{11} and e_{13} values (unit: 10^{-10} C/m). The inset shows top view of the 2 x 2 x 1 supercell structure of 2H VSSe monolayer.

In conclusion, by using first-principles and particle swarm search approaches compensated with a $k \cdot p$ model, we predicted a new magnetic Janus monolayer VSSe with novel multi-ferroic properties which can persist at room temperature. The broken space inversion guarantees the inequivalent Berry curvature, and the spin-valley coupling leads to time-reversal violation, thus the valley polarization can be realized in magnetic Janus VSSe. Moreover, ferroelasticity with a huge reversal strain (73%) can be achieved in magnetic Janus VSSe. Most interestingly, the coupling between electric polarization and mechanical strain can result in a giant in-plane piezoelectric polarization. Our results highlighted a new interesting magnetic 2D Janus VSSe monolayer that can combine ferromagnetism, ferroelasticity, piezoelectric effect, and valley polarization, offering advantages over other 2D materials for potential applications in nanoelectronics, optoelectronics and valleytronics.

Corresponding Author

Aijun Du, Email: aijun.du@qut.edu.au

A.D acknowledges the financial support by Australian Research Council under Discovery Project (DP170103598) and computer resources provided by high-performance computer time from

computing facility at the Queensland University of Technology, NCI National Facility, and the Pawsey Supercomputing Centre through the National Computational Merit Allocation Scheme supported by the Australian Government and the Government of Western Australia.

References

[1] D.-W. Fu *et al.*, Science **339**, 425 (2013).
[2] C. Huang, Y. Du, H. Wu, H. Xiang, K. Deng, and E. Kan, Phys. Rev. Lett. **120**, 147601 (2018).
[3] W. Eerenstein, N. Mathur, and J. F. Scott, Nat. **442**, 759 (2006).
[4] M. Wu and X. C. Zeng, Nano Lett. **17**, 6309 (2017).
[5] A.-Y. Lu *et al.*, Nat. Nanotechnol. **12**, 744 (2017).
[6] Z. L. Wang and J. Song, Science **312**, 242 (2006).
[7] W. Wu *et al.*, Nat. **514**, 470 (2014).
[8] H. Zhu *et al.*, Nat. Nanotechnol. **10**, 151 (2015).
[9] R. Li, Y. Cheng, and W. Huang, Small, 1802091 (2018).
[10] D. Xiao, W. Yao, and Q. Niu, Phys. Rev. Lett. **99**, 236809 (2007).
[11] R. Peng, Y. Ma, S. Zhang, B. Huang, and Y. Dai, J. Phys. Chem. Lett. (2018).
[12] M. Bonilla *et al.*, Nat. Nanotechnol. **13**, 289 (2018).
[13] M. Wu and X. C. Zeng, Nano Lett. **16**, 3236 (2016).
[14] Y. Wang, J. Lv, L. Zhu, and Y. Ma, Phys. Rev. B **82**, 094116 (2010).
[15] G. Kresse and J. Hafner, Phys. Rev. B **47**, 558 (1993).
[16] G. Kresse and J. Furthmüller, Phys. Rev. B **54**, 11169 (1996).
[17] P. E. Blöchl, Phys. Rev. B **50**, 17953 (1994).
[18] J. Heyd, G. E. Scuseria, and M. Ernzerhof, J. Chem. Phys. **118**, 8207 (2003).
[19] S. Grimme, J. Comput. Chem. **27**, 1787 (2006).
[20] K. Parlinski, Z. Li, and Y. Kawazoe, Phys. Rev. Lett. **78**, 4063 (1997).
[21] A. Togo, F. Oba, and I. Tanaka, Phys. Rev. B **78**, 134106 (2008).
[22] R. King-Smith and D. Vanderbilt, Phys. Rev. B **47**, 1651 (1993).
[23] J. Zhang *et al.*, ACS nano **11**, 8192 (2017).
[24] L. Ke, B. N. Harmon, and M. J. Kramer, Phys. Rev. B **95**, 104427 (2017).
[25] L. Ke, M. van Schilfgaarde, and V. Antropov, Phys. Rev. B **86**, 020402 (2012).
[26] C. Gong *et al.*, Nat. **546**, 265 (2017).
[27] B. Huang *et al.*, Nat. **546**, 270 (2017).
[28] W.-Y. Tong, S.-J. Gong, X. Wan, and C.-G. Duan, Nat. Commun. **7**, 13612 (2016).
[29] X. Wang *et al.*, Sci. Adv. **2**, e1600209 (2016).